ORIGINAL ARTICLE

Mathematical Model of Pulsed Immunotherapy for Superficial Bladder Cancer

Svetlana Bunimovich-Mendrazitsky[a,*], Helen Byrne[b], Lewi Stone[a]

[a] *Biomathematics Unit, Department of Zoology, Faculty of Life Science, Tel-Aviv University, Tel-Aviv 69978, Israel*
[b] *Centre for Mathematical Medicine and Biology, School of Mathematical Sciences, Nottingham, NG7 2RD, UK*

Abstract We present a theoretical study of superficial bladder cancer growth and its treatment via pulsed immunotherapy with *Bacillus Calmette–Guérin* (BCG), an attenuated strain of *Mycobacterium bovis*. BCG pulsed immunotherapy is a clinically established procedure for the treatment of superficial bladder cancer. In this paper, periodic BCG instillations are modeled using impulsive differential equations, which are studied using a combination of analytical and numerical techniques. In this way, we determine critical threshold values of the BCG instillation dose and rate of pulsing for successful treatment. We also identify treatment regimes in which tumor destruction occurs, but undesirable side effects are maintained at low levels by the immune system.

1. Introduction

Bladder cancer is a world-wide problem, being the fourth most common cancer among men and the eighth most common cancer among women (Meyer et al., 2002). Its incidence is increasing in industrialized and developed countries whereas the mortality rate remains largely unchanged (Chopin and Gattegno, 2002). Bladder cancer is an aggressive disease with fatal consequences. Untreated it slowly grows, first into the bladder wall and then out into the abdomen and nearby organs, such as the prostate, vagina, uterus, and rectum.

The most common cancer of the bladder, Transitional Cell Carcinoma (TCC), originates from the transitional epithelium (part of the urothelium) that lines the bladder cavity. TCC has been classified into two types depending on the depth of penetration and risk of progression (see Fig. 1):
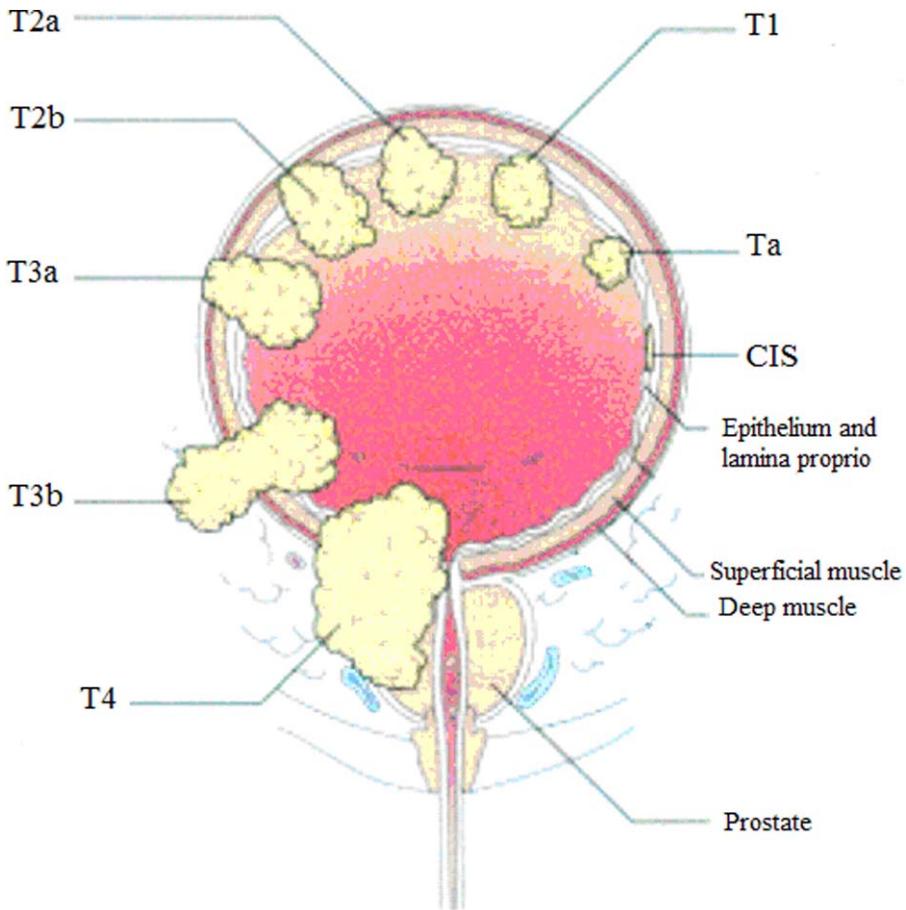

Fig. 1 Stages of bladder cancer from (Meyer et al., 2002). Bladder cancer can be divided into superficial and muscle invasive cancer. Superficial bladder cancer penetrates the bladder wall no deeper than the epithelial tissue and lamina proprio—Ta, T1 stages, and CIS

(a) Superficial bladder cancer includes low-grade papillary TCC (stages Ta and T1) and carcinoma in situ (CIS). Growth occurs superficially on the inner surface of the bladder in the form of a polyp but does not extend to the muscle. Of patients presenting with TCC, 50% are in stage Ta, 20% in T1, and 5% CIS (Chopin and Gattegno, 2002; Bevers et al., 2004; Schenkman and Lamm, 2004).

(b) Invasive bladder cancer consists of high-grade TCC (stages T2–T4) and affects about 25% of patients presenting with TCC. Here, the cancer invades the surrounding muscle and tissue, causing metastatic disease. Treatment often requires removal of the bladder (cystectomy) to prevent the tumor from spreading to the lungs, liver, and bone (Nseyo and Lamm, 1997).

The preferred treatment for bladder cancer depends on its grade at diagnosis. For superficial bladder cancer, local surgery is applied first. Small regions of cancerous tissue are

removed through the urethra, using a local procedure called transurethral resection (TUR). During TUR, the doctors also remove a small piece of polyp for microscopic examination (biopsy). In the case of malignant tissue (indicating the tumor is in progression), the treatment is either chemotherapy or immunotherapy for eradication of any residual cancer cells.

Intravesical *Bacillus Calmette–Guérin* (BCG) is a type of immunotherapy that is used to treat superficial bladder cancer. BCG is an attenuated nonpathogenic strain of *Mycobacterium bovis* that was originally used as a vaccine against tuberculosis. In this treatment, bacterial instillations are introduced into the bladder with a lighted tube (catheter) that is inserted through the urethra. After instillation, BCG accumulates near the bladder wall, and in superficial tumor cells. On binding to the cell wall, BCG is internalized and processed by both antigen-presenting cells (APC) and uninfected tumor cells. BCG antigens stimulate a strong immune response characterized by a surge in cytokine levels in infected areas and in the urine. The cytokine cascade stemming from the APCs activates a variety of cells including cytotoxic T cells (CTL), lymphocyte-activated killer (LAK) (Schenk-Braat and Bangma, 2005), and natural killer cells (NK) (Bohle and Brandau, 2003), which ultimately kill the BCG-infected tumor cells (Patard et al., 1998) and eliminate the entire tumor.

Current practice involves administering weekly intravesical instillations of BCG over a 6-week period for low-risk tumor progression and for up to 9 weeks for high-risk tumor progression (Chopin and Gattegno, 2002). Presently, pulsed BCG treatment of TCC works best for superficial bladder cancer, although it is not completely effective. For example, even after treatment with BCG, the probability that new tumors will develop in other areas of the bladder over the next ten years is 75%. Additionally, 10% of patients who receive BCG treatment experience side effects, while another 5% develop BCG sepsis in which bacteria or other toxins are found in the blood or other tissues of the body (Alexandroff et al., 1999). Other side effects associated with BCG include high fever, general malaise and chills, persistent bladder infection, lung infection, and liver toxicity (Kim and Steinberg, 2001).

As with any biological therapy, the response to BCG is not linear, and hence changing dosing schedules may unexpectedly cause adverse side-effects, leading to an interruption in the course of treatment (Zlotta et al., 2000). In addition, a large BCG dose may suppress the maximum induction of cytokines and adhesion molecules (Alexandroff et al., 1999). After trying BCG protocols (Ojea et al., 2007) to improve the response Schenkman and Lamm (2004) concluded that it is difficult to define the optimal protocol of BCG immunotherapy.

Our modeling approach is similar to that of Kuznetsov et al. (1994), Panetta (1996), Kirschner and Panetta (1998), Lakmeche and Arino (2001), De Pillis et al. (2005, 2006), although none of these authors studied bladder cancer or pulsing immunotherapy treatment. In Bunimovich-Mendrazitsky et al. (2007), the first mathematical model describing tumor-immune interactions in the bladder as a result of continuous BCG therapy was developed. The aim in the present paper is to adapt their model in order to provide insights into the dynamic processes that occur when BCG immunotherapy is administered as a sequence of pulsed instillations.

2. Mathematical model

The following model is based on pulsed administration of BCG therapy for the treatment of superficial TCC of the urinary bladder. It extends a model originally developed by Bunimovich-Mendrazitsky et al. (2007) to describe continuous administration of BCG therapy. The earlier model admits three types of equilibria when the growth rate of the tumor cells is taken to be logistic:

(I) Tumor-equilibrium—here persistence of the tumor indicates failure of the BCG treatment;
(II) Tumor-free equilibrium—here the tumor is eradicated, with only transient side effects;
(III) Side-effects equilibrium—here the tumor is eradicated but a persistent immune response is elicited.

The existence and stability of these steady states depend on biologically relevant parameters and the size of the tumor at the start of treatment. For most parameter ranges, one locally stable equilibrium exists, although cases of coexistence can occur. Conditions for local stability and bistability are detailed in Bunimovich-Mendrazitsky et al. (2007). In the worst case scenario, where the growth rate of cancer cells is taken to be exponential, the model has no stable equilibria and unbounded tumor growth is predicted. In this paper, we focus on pulsed BCG treatment, rather than continuous infusion, using impulsive differential equations to model the pulsed treatment (see, e.g., Lakshmikantham et al., 1989; Bainov, 1993; Shulgin et al., 1998; Stone et al., 2000). We aim to establish criteria for successful BCG treatment.

As stated above, the model that we develop describes interactions between BCG, the immune system and tumor cells within the bladder (see Fig. 2). There are four key variables of interest:

- $B(t)$—the concentration of BCG in the bladder;
- $E(t)$—the concentration of activated immune-system or *effector* cells, that are toxic to the tumor infected cells.
- The tumor cells are divided into two subpopulations:
  - $T_u(t)$—those that are uninfected;
  - $T_i(t)$—those that have been infected with BCG.

To simplify the model, we group the immune cells (APC, CTL, NK, LAK) into a single population of cells which we term effector cells (E). They target and destroy infected tumor cells (T_i). The latter decrease at a rate proportional to that at which they encounter effector cells. Assuming random mixing, the encounter rate is proportional to the product $p_3 E T_i$, where p_3 is a rate constant. Similarly, tumor cells become infected with BCG at rate $p_2 B T_u$ where p_2 is a rate coefficient. Thus, the dynamics of the two tumor populations are given by:

$$\frac{dT_i}{dt} = -p_3 E T_i + p_2 B T_u,$$

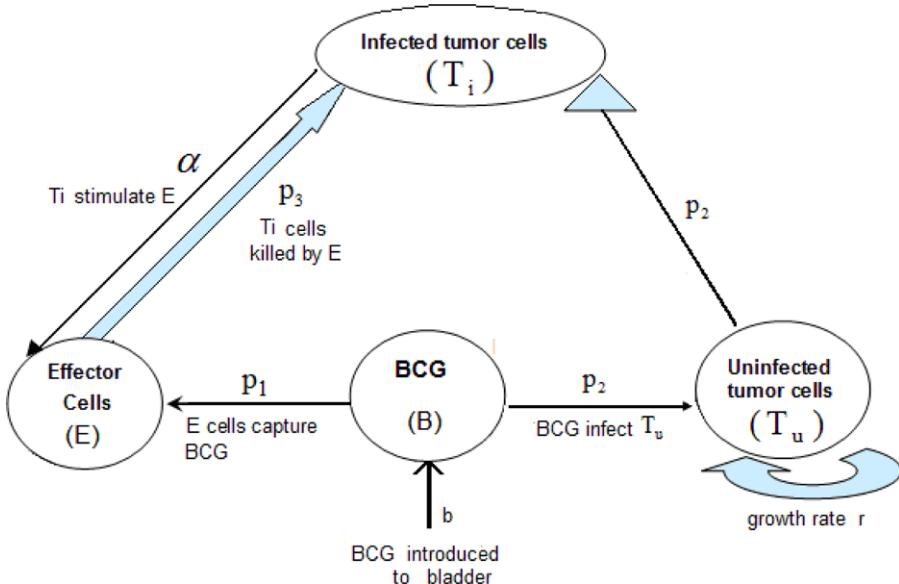$$\frac{dT_u}{dt} = -p_2 B T_u + r T_u.$$

Fig. 2 Schematic diagram of the model illustrating how tumor cell eradication by BCG may occur in superficial bladder cancer

In the above equations, we have assumed that in the absence of BCG uninfected tumor cells T_u undergo exponential growth, with growth rate r.

We assume that a BCG instillation of quantity b is injected into the bladder every τ time units. By modeling the instillation as a Dirac delta-function, $b\delta(t - n\tau)$ we ensure that the nth dose raises $B(t)$ by exactly b units at time $t = n\tau$. As stated above, free BCG binds to malignant urothelial tumor cells, infecting them at rate p_2 (De Boer et al., 1996; Durek et al., 1999). BCG is lost as a result of both natural decay (with half life of μ_1^{-1}) and interactions with macrophages and dendritic cells (APC), and natural killer cells (NK) (Wigginton and Kirschner, 2001), which we are treating collectively as effector cells, E. We therefore assume that this loss occurs at rate $p_1 EB$ where p_1 is a positive rate constant. Combining this ideas we arrive at the following evolution equation for $B(t)$:

$$\frac{dB}{dt} = -\mu_1 B - p_1 EB - p_2 BT_u + \sum_{n=0}^{\infty} b\delta(t - n\tau).$$

Factors influencing the number of effector cells are: the rate at which they are recruited from the bone marrow by infected tumor cells (αT_i), encounters between immune cells and BCG ($p_4 EB$), their natural cell death rate (μ_2), and the rate at which they are absorbed by infected tumor cells ($p_5 ET_i$). Therefore, the dynamics of the immune system is modeled by the following differential equation:

$$\frac{dE}{dt} = -\mu_2 E + \alpha T_i + p_4 EB - p_5 ET_i.$$

The ordinary differential equations for T_i, T_u, B, and E stated above constitute our mathematical model. Before continuing, it is helpful to cast them in terms of dimensionless units (see Appendix C). The following system of nondimensional ordinary differential equations is obtained:

$$
\begin{aligned}
\frac{dB}{dt} &= -B(1 + p_1 E + p_2 T_u) + \sum_{n=0}^{\infty} b\delta(t - n\tau), \\
\frac{dE}{dt} &= E(-\mu + p_4 B - p_5 T_i) + \alpha T_i, \\
\frac{dT_i}{dt} &= -p_3 E T_i + p_2 B T_u, \\
\frac{dT_u}{dt} &= -p_2 B T_u + r T_u.
\end{aligned}
\tag{1}
$$

We impose the following initial conditions:

$$
B(0) = b, \qquad E(0) = T_i(0) = 0, \qquad T_u(0) > 0,
\tag{2}
$$

where b represents the dose of BCG administrated in each instillation.

Those model parameters which can be estimated from biological data are summarized in Appendix C and based on values described in Bunimovich-Mendrazitsky et al. (2007). We emphasize that dimensionless units will be used throughout the model analysis that follows unless stated explicitly otherwise.

3. Numerical simulations

Equations (1) were solved numerically using a fourth order Runge–Kutta scheme. Figure 3a shows a typical simulation for a treatment protocol in which BCG instillations of strength $b = 0.2$ are applied every $\tau = 7$ days (see Table A.1, Appendix C for a full list of parameter values). For this choice of parameter values, the uninfected tumor cells T_u are eventually eliminated, and the system converges to a state that is akin to the tumor-free equilibrium described in Bunimovich-Mendrazitsky et al. (2007), with $E^* = T_i^* = T_u^* = 0$. (Here we use superscripts "*" when referring to equilibrium values.) The BCG variable $B(t)$, on the other hand, remains periodic in time (see Fig. 3).

Figure 3 makes clear that the parameters b and τ have significant control on the dynamics of the pulsed system. Figure 3b shows that less frequent pulsing ($\tau = 19$ days rather than $\tau = 7$ days) for the same strength of BCG (i.e., $b = 0.2$) as in Fig. 3a, may cause treatment to fail: the tumor continues to grow and, in the long term, the number of effector cells eventually falls to zero. The simulation presented in Fig. 3c shows how increasing the BCG dose from $b = 0.2$ to $b = 1.25$ (with $\tau = 7$ as in Fig. 3a) leads to a large and persistent effector cell population, a situation which we term a "side-effect" state.
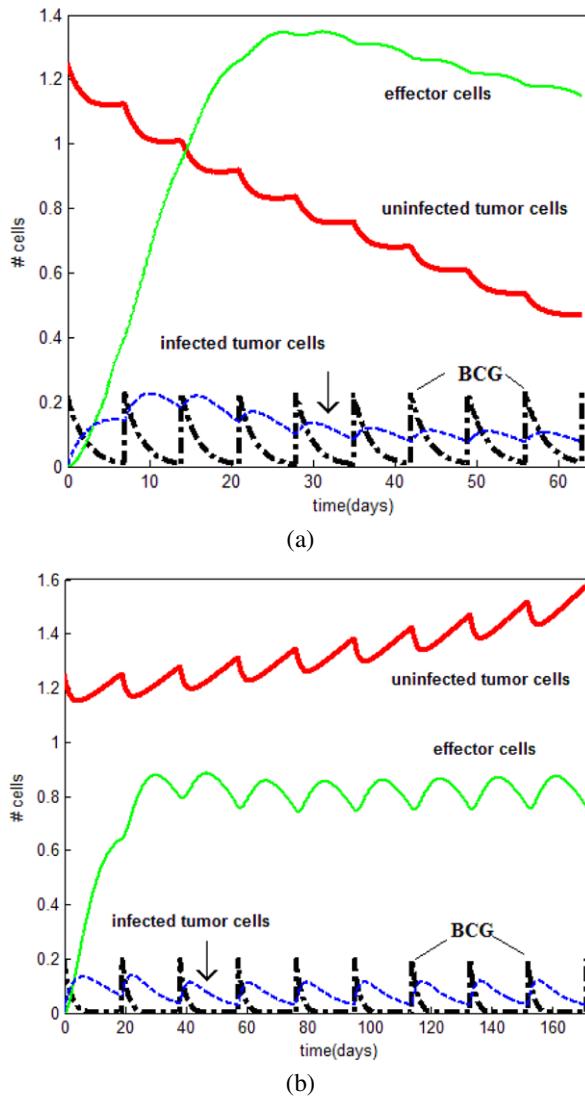
(a)

(b)

Fig. 3 Series of simulations showing how changing the frequency (τ^{-1}) and strength (b) of the BCG instillations affects the system dynamics. (a) When $\tau = 7$ days and $b = 0.2$ treatment is successful, the tumor is eliminated and immune response eventually dies away; (b) when $\tau = 19$ days and $b = 0.2$, the immune response is not strong enough to eliminate the tumor which grows unboundedly; (c) when $\tau = 7$ and $b = 1.25$, the tumor is eliminated, but a strong and persistent immune response is elicited. Key: un-infected tumor cells (solid heavy line), effector cells (solid line), tumor cells infected with BCG (dashed line) and BCG (dash-dotted line; concentration). Parameter values: as per Table A.1 with initial tumor size before treatment $T_u(0) = 1.25$
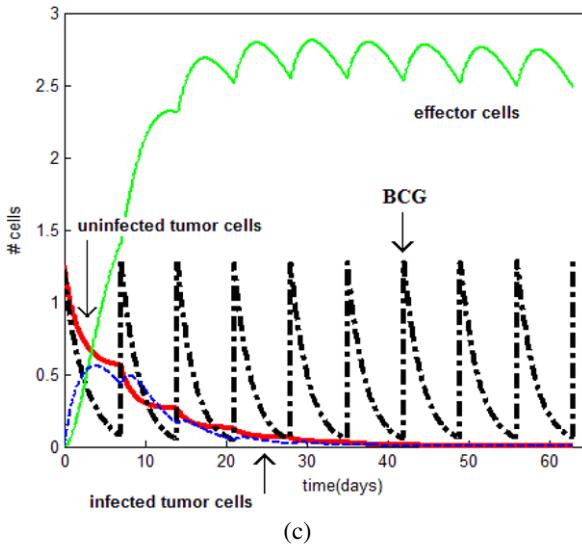
(c)

Fig. 3 (*Continued*)

4. The periodic "tumor-free" solution

Guided by the numerical results presented in Fig. 3a, showing successful elimination of the tumor cells, we start our analysis of Eq. (1) by demonstrating the existence of a periodic "*tumor-free*" limit cycle. By observation, we note that Eq. (1) admits the following solution $E^* = T_i^* = T_u^* = 0$, with the BCG dynamics satisfying

$$\frac{dB}{dt} = -B + \sum_{n=0}^{\infty} b\delta(t - n\tau). \tag{3}$$

The delta function formulation allows us to determine the dynamics between consecutive pulses at $t = n\tau$ and $t = (n+1)\tau$:

$$\frac{1}{B}\frac{dB}{dt} = -1, \quad n\tau \leq t < (n+1)\tau,$$

with $[B]_{n\tau^-}^{n\tau^+} = b$. If, in addition, the initial conditions are such that $B(0) = b$, then the solution is given by:

$$B(t) = B(0)e^{-t} = be^{-t}, \quad 0 \leq t < \tau,$$

$$B(t) = \left(be^{-\tau} + b\right)e^{-(t-\tau)}, \quad \tau \leq t < 2\tau,$$

$$\vdots$$

$$B(t) = \left(B(n\tau^-) + b\right)e^{-(t-n\tau)} = \frac{b(1 - e^{-(n+1)\tau})}{(1 - e^{-\tau})}e^{-(t-n\tau)}, \quad n\tau \leq t < (n+1)\tau.$$

In the limit of large n, $B(t)$ converges to a periodic cycle denoted by $\tilde{B}(t)$, and the associated infection free state may be described as:

$$\tilde{B}(t) = \frac{b e^{-(t-n\tau)}}{1 - e^{-\tau}}, \quad n\tau \le t < (n+)\tau,$$
$$E^* = T_i^* = T_u^* = 0. \tag{4}$$

5. Stability of the periodic "tumor-free" solution

The stability of the limit cycle solution identified above may be studied by introducing a small parameter $\varepsilon \ll 1$ and linearizing system (1) about the limit cycle solution (4) so that:

$$
\begin{aligned}
B(t) &= \tilde{B}(t) + \varepsilon B_1 + \varepsilon^2 B_2 + \cdots, \\
E(t) &= \varepsilon E_1 + \varepsilon^2 E_2 + \cdots, \\
T_i(t) &= \varepsilon T_{i1} + \varepsilon^2 T_{i1} + \cdots, \\
T_u(t) &= \varepsilon T_{u1} + \varepsilon^2 T_{u2} + \cdots.
\end{aligned}
\tag{5}
$$

The linearization involves inserting (5) into the ODE system (1), equating coefficients of $O(\varepsilon)$ to zero and neglecting terms of $O(\varepsilon^2)$. For clarity of notation, in what follows, we omit the subscripts, writing $B = B_1, E = E_1, T_i = T_{i1}, T_u = T_{u1}$ to describe the $O(\varepsilon)$ terms. In this way, for $n\tau \le t < (n+1)\tau$, we obtain:

$$
\begin{aligned}
\frac{dB}{dt} &= -B - p_1 E \tilde{B}(t) - p_2 T_u \tilde{B}(t), \\
\frac{dE}{dt} &= E\big(-\mu + p_4 \tilde{B}(t)\big) + \alpha T_i, \\
\frac{dT_i}{dt} &= p_2 \tilde{B}(t) T_u, \\
\frac{dT_u}{dt} &= -p_2 \tilde{B}(t) T_u + r T_u.
\end{aligned}
\tag{6}
$$

Equations (6) constitute a system of linear differential equations with periodic coefficients. As such, they can be analyzed using the Floquet theory (for details, see Appendix B). The first step involves constructing the fundamental matrix $\underline{\underline{Y}}(t)$ (Zwillinger, 1989):

$$
\underline{\underline{Y}}(t) =
\begin{bmatrix}
B_1(t) & B_2(t) & B_3(t) & B_4(t) \\
E_1(t) & E_2(t) & E_3(t) & E_4(t) \\
T_{i1}(t) & T_{i2}(t) & T_{i3}(t) & T_{i4}(t) \\
T_{u1}(t) & T_{u2}(t) & T_{u3}(t) & T_{u4}(t)
\end{bmatrix},
$$

where $(B_j(t), E_j(t), T_{ij}(t), T_{uj}(t)) \, j = [1; 4]$ are independent solutions of the linear system (6). These solutions are obtained by choosing initial conditions $(B_j(0), E_j(0), T_{ij}(0), T_{uj}(0)) \, j = [1; 4]$: so that $\underline{Y}(0) = \underline{I}$. Solving Eq. (6) for these initial conditions gives:

$$\left(B_1(t), E_1(t), T_{i1}(t), T_{u1}(t)\right) = \left(e^{-t}, 0, 0, 0\right),$$

$$\left(B_2(t), E_2(t), T_{i2}(t), T_{u2}(t)\right) = \left(B_2(t), e^{-\mu t + \frac{bp_4}{1-e^{-\tau}}(1-e^{-t})}, 0, 0\right),$$

$$\left(B_3(t), E_3(t), T_{i3}(t), T_{u3}(t)\right) = \left(B_3(t), E_3(t), 1, 0\right),$$

$$\left(B_4(t), E_4(t), T_{i4}(t), T_{u4}(t)\right) = \left(B_4(t), E_4(t), T_{i4}(t), e^{rt - \frac{p_2 b}{1-e^{-\tau}}(1-e^{-t})}\right).$$

We do not state the exact forms of $B_2(t), B_3(t), B_4(t), E_3(t), E_4(t), T_{i4}(t)$ here since their precise form does not affect our analysis.

Given that $t = \tau$ represents the period of the coefficients, the "Floquet multipliers" are defined as the eigenvalues λ of the matrix $\underline{Y}(\tau)$:

$$\text{Det}\left(\underline{Y}(\tau) - \lambda\underline{I}\right) = \text{Det}\begin{bmatrix} e^{-\tau} - \lambda & B_2(\tau) & B_3(\tau) & B_4(\tau) \\ 0 & e^{-\mu\tau + p_4 b} - \lambda & E_3(\tau) & E_4(\tau) \\ 0 & 0 & 1 - \lambda & T_{i4}(\tau) \\ 0 & 0 & 0 & e^{r\tau - p_2 b} - \lambda \end{bmatrix} = 0.$$

Since $Y(\tau)$ is upper triangular, the Floquet multipliers are:

$$\lambda_1 = e^{-\tau} < 1, \qquad \lambda_2 = e^{-\mu\tau + p_4 b}, \qquad \lambda_3 = 1, \qquad \lambda_4 = e^{r\tau - p_2 b}. \tag{7}$$

According to Floquet theory, the absolute value of one of the multipliers is equal to unity (Glendinning, 1994), and the tumor-free limit cycle associated with system (4) is locally stable if the absolute values of all other Floquet multipliers are less than unity. Stability thus requires that:

$$|\lambda_2| = e^{-\mu\tau + p_4 b} < 1 \quad \text{and} \quad |\lambda_4| = e^{r\tau - p_2 b} < 1.$$

We deduce that the periodic "tumor-free" solution under BCG-pulse therapy is locally stable if the BCG dose b for a given value of τ lies within a finite range:

$$\frac{r}{p_2} < \frac{b}{\tau} < \frac{\mu}{p_4}, \tag{8}$$

where $\frac{b}{\tau}$ is the average dose of BCG administrated per unit time. The eradication of the tumor thus depends on two key biological ratios $\frac{r}{p_2}$ and $\frac{\mu}{p_4}$:

(a) $\frac{r}{p_2}$ is the ratio of the growth rate (r) of the tumor to the rate at which BCG infects the tumor cells (p_2). If for a fixed value of τ, this ratio exceeds the effective rate of BCG influx $\frac{b}{\tau}$, then the tumor-free equilibrium loses stability. This lower bound on $\frac{b}{\tau}$ shows how competition between the BCG infection rate and the tumor growth rate affects a tumor's response to BCG-pulse therapy.
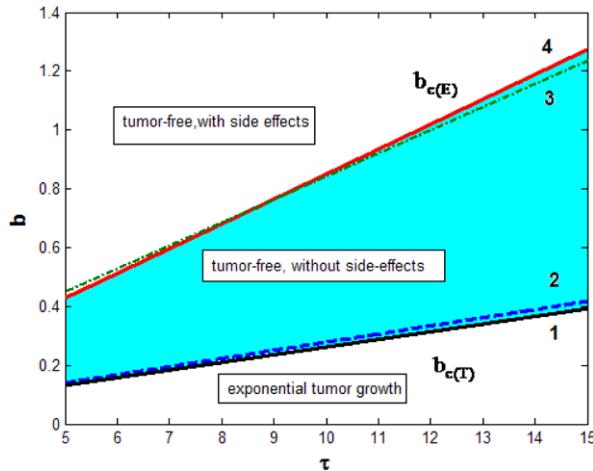
Fig. 4 Diagram showings how the outcome following pulsed BCG therapy depends on the dose (b) and period of pulsing (τ). Theoretical predictions are represented by dashed lines and simulations by solid lines. *Curve 1*: theoretically-determined curve showing how $b_{c(T)}$ varies with τ (see Eq. (11)). *Curve 2*: numerically-determined curve showing how $b_{c(T)}$ varies with τ. *Curve 3*: numerically-determined curve showing how $b_{c(E)}$ varies with τ. *Curve 4*: theoretically-determined curve showing how $b_{c(E)}$ varies with τ (see Eq. (13)). Parameter values as per Table A.1, with $T_u(0) = 0.02$

(b) $\frac{\mu}{p_4}$ is the ratio of the mortality rate of effector cells (μ) to the rate at which they are recruited (p_4). If this ratio is smaller than the effective BCG influx, $\frac{b}{\tau}$ than the immune system will remain switched on ($E > 0$).

Equivalently, we can consider $b_{c(T)} = \frac{r\tau}{p_2}$ as the minimal BCG dose for which tumor eradication occurs, and $b_{c(E)} = \frac{\mu\tau}{p_4}$ as the maximal BCG dose which does not cause an excessive and persistent immune response (E). The two thresholds imply that doses of BCG that are too large or too small ($b < \frac{r\tau}{p_2}$ or $b > \frac{\mu\tau}{p_4}$) will result in exponential growth in the size of the tumor or have a detrimental effect on the immune system (see Figs. 3a and 3c).

In Fig. 4, we use Eq. (8) to show how the critical values of b vary with the pulsing time τ. We note that as τ (i.e., the time interval between installations) increases, the minimum dosage $b_{c(T)}$ needed to exceed the threshold and eliminate the tumor also increases. We note also that the theoretical results are in good agreement with numerical simulations of Eq. (1). These simulations were obtained using initial conditions close to the tumor-free state, a point that is discussed further below.

6. Interpreting the threshold criteria

The threshold conditions (8) derived above give little insight into their origins. The analysis presented below provides a more intuitive interpretation of the stability conditions. Consider first the linearized tumor dynamics in Eq. (6)

$$\frac{dT_u}{dt} = -p_2 \tilde{B}(t) T_u + r T_u,$$

where $\tilde{B}(t)$ is specified in Eq. (4). Between any two BCG pulses $n\tau \leq t \leq (n+1)\tau$, we have:

$$\frac{dT_u}{dt} = T_u\left(r - p_2\frac{be^{-(t-n\tau)}}{1 - e^{-\tau}}\right), \quad n\tau < t < (n+1)\tau. \tag{9}$$

If we introduce $R = r\tau - p_2 b$, then it is possible to show that:

$$
\begin{aligned}
& T_u(\tau) = T_u(0)e^R, \\
& T_u(2\tau) = T_u(\tau)e^R = T_u(0)e^{2R}, \\
& \vdots \\
& T_u((n+1)\tau) = F\big[T_u(n\tau)\big], \quad \text{where } F\big[T_u(n\tau)\big] = T_u(n\tau)e^R,
\end{aligned}
\tag{10}
$$

The stroboscopic map $F(T_u)$ has a fixed point $T_u^* = F(T_u^*) = 0$, which is stable if:

$$|F'(T_u^*)| = e^R < 1.$$

Thus, the criterion for tumor eradication becomes $R < 0$ or equivalently:

$$b > b_{c(T)} = \frac{r\tau}{p_2}. \tag{11}$$

Similarly, the linearized dynamics of the bacterial-immune system, specified by Eq. (6) may be approximated as:

$$\frac{dE}{dt} = E\big(-\mu + p_4\tilde{B}(t)\big).$$

In obtaining the above equation, we have assumed that $\alpha \ll 1$ and the number of infected-tumor cells remains close to the equilibrium value $T_i^* = 0$. Substituting with $\tilde{B}(t)$ from Eq. (4), we deduce that:

$$\frac{dE}{dt} = E\left(-\mu + p_4\frac{be^{-(t-n\tau)}}{1 - e^{-\tau}}\right), \quad n\tau \leq t < (n+1)\tau.$$

If we introduce $P = p_4 b - \mu\tau$, then it is possible to show that $E(n\tau)$ satisfies the stroboscopic map:

$$E\big((n+1)\tau\big) = F\big[E(n\tau)\big], \quad \text{where } F\big[E(n\tau)\big] = E(n\tau)e^P.$$

The map $F(E)$ has a fixed point $E^* = F(E^*) = 0$, which is stable if:

$$\left|\frac{dF(E^*)}{dE}\right| = e^{(-\mu\tau + p_4 b)} < 1. \tag{12}$$

This will be the case if:

$$b < b_{c(E)} = \frac{\mu\tau}{p_4}, \tag{13}$$

where $b_{c(E)}$ is the critical BCG therapy level. Note that if $b < b_{c(E)}$, then the immune system will be regulated after treatment and E will eventually reduce to its equilibrium state zero. (Thus, the plot of E in Fig. 3a will eventually converge to zero.) If $b > b_{c(E)}$, then the effector cell population ($E^* > 0$) increases in size and persists at long times. The behavior of the immune system in this case is depicted in Fig. 3c.

The shaded triangle in Fig. 4 highlights those values of BCG dose and frequency from condition (8), yielding a state that is tumor-free ($T_u^* = 0$) and without effector cells ($E^* = 0$). Doses of BCG outside this region result in either exponential growth of the tumor or have a detrimental effect on the immune system.

7. Effect of initial tumor size

The Floquet analysis presented in Section 5 yields information about local stability and is based on the assumption that initially the system is close to the tumor-free equilibrium, with $T_u(0) \approx 0$. However, if the initial tumor size is large, the threshold predictions may be affected significantly. Numerical simulations suggest that if $T_u(0)$ is sufficiently large then the tumor-free limit cycle may never be reached, even though it is locally stable. Apart from the periodic tumor-free limit cycle discussed above, it is possible to identify a solution for which $B(t) \to 0$, while $T_u(t)$ continues to grow exponentially. In fact, there is a separatrix, which demarcates the basin of attraction of the trivial tumor-free solution and the solution for which the tumor grows unboundedly. If $T_u(0)$ is sufficiently small such that the initial condition lies below the separatrix then the system is attracted to the tumor-free equilibrium (see Fig. 3a). Equally, if $T_u(0)$ is initially large enough, such that the system is above the separatrix, then the tumor grows uncontrollably (Fig. 3b).

We investigate this dependence on initial conditions as follows. First, we suppose that initially the immune system is unstimulated ($E(0) = 0$), so that there are no infected tumor cells ($T_i(0) = 0$) and that the tumor is large so that $T_u(0) \gg 1$. Now we seek to identify the critical parameter value of b^*, such that for $b < b^*$ the tumor grows unboundedly ($T_u \to \infty$ as $t \to \infty$), and for $b > b^*$ the tumor regresses ($T_u \to 0$, as $t \to \infty$). This critical value of b delineates the switch between tumor extinction and exponential growth.

We make analytical progress by introducing the small parameter $\delta \ll 1$ and assuming that treatment starts when $T_u = \frac{\widehat{T_u}(t)}{\delta} \gg 1$ and $E = \delta \widehat{E}(t) \ll 1$. Inserting these rescalings into the dimensionless Eqs. (1), we deduce that B, $\widehat{E}$, $\widehat{T_u}$ and T_i satisfy:

$$
\begin{aligned}
\frac{dB}{dt} &= -B\left(1 + \frac{p_2 \widehat{T_u}}{\delta} + \delta p_1 \widehat{E}\right), \\
\frac{d\widehat{E}}{dt} &= \widehat{E}(-\mu + p_4 B - p_5 T_i) + \frac{\alpha T_i}{\delta}, \\
\frac{dT_i}{dt} &= -\delta p_3 T_i \widehat{E} + \frac{p_2}{\delta} \widehat{T_u} B, \\
\frac{d\widehat{T_u}}{dt} &= (r - p_2 B)\widehat{T_u}.
\end{aligned}
\tag{14}
$$

Note that the ODEs for B, $\widehat{E}$, and T_i are singular in the limit as $\delta \to 0$, indicating that there is a short timescale over which these variables change. We determine this behavior

by rescaling time so that $t^* = t/\delta$ in which case Eqs. (14) become:

$$\frac{dB}{dt^*} = -B\left(\delta + p_2\widehat{T}_u + \delta^2 p_1\widehat{E}\right),$$

$$\frac{d\widehat{E}}{dt^*} = \alpha T_i + \delta\widehat{E}(-\mu + p_4 B - p_5 T_i),$$

$$\frac{dT_i}{dt^*} = -\delta^2 p_3 T_i \widehat{E} + p_2\widehat{T}_u B,$$

$$\frac{d\widehat{T}_u}{dt^*} = \delta(r - p_2 B)\widehat{T}_u.$$

(15)

We then seek a power series expansion of the form:

$$B(t^*) = B_0(t^*) + \delta B_1(t^*) + \cdots,$$

$$\widehat{E}(t^*) = \widehat{E}_0(t^*) + \delta\widehat{E}_1(t^*) + \cdots,$$

$$T_i(t^*) = T_{i0}(t^*) + \delta T_{i1}(t^*) + \cdots,$$

$$\widehat{T}_u(t^*) = \widehat{T}_{u0}(t^*) + \delta\widehat{T}_{u1}(t^*) + \cdots.$$

Our main aim is to determine value of b, which separates parameter space into regions in which tumor growth is exponential and regions in which the tumor decays. Since $\frac{d\widehat{T}_u}{dt^*} = O(\delta)$, we deduce that $\widehat{T}_{u0}(t^*) = T_{u0}^*$ is constant for all t^*.

Equating to zero terms of $O(\delta)$ we deduce that $\widehat{T}_{u1}(t^*)$ solves:

$$\frac{d\widehat{T}_{u1}}{dt^*} = (r - p_2 B_0)T_{u0}^*.$$

(16)

Solving the above ODE requires knowledge of B_0. Turning now, then, to the ODE for B_0, we find by equating to zero coefficients of $O(1)$ that B_0 solves:

$$\frac{dB_0}{dt^*} = -p_2 T_{u0}^* B_0, \quad n\tau^* \leq t^* < (n+1)\tau^*.$$

Hence,

$$B_0(t^*) = B_0(n\tau^*)^+ \exp\left[-p_2 T_{u0}^*(t^* - n\tau^*)\right],$$

(17)

where the symbol "+" designates that we are referring to the concentration of bacteria B_0 instantaneously *after* a pulse is administered.

We deduce further that when the $(n+1)$th pulse is administered (at time $t^* = (n+1)\tau^{*+}$):

$$B_0\left[(n+1)\tau^*\right]^+ = B_0(n\tau^*)^+ \exp(-p_2 T_{u0}^*\tau^*) + b.$$

We look for a periodic solution of B_0 and thus set $B[(n+1)\tau^*]^+ = B(n\tau^*)^+$, which gives:

$$B_0(n\tau^*)^+ = \frac{b}{1 - e^{-p_2 T_{u0}^*\tau^*}}.$$

(18)

Returning now to Eq. (16), on substituting from (17) for $B_0(t^*)$, we arrive at:

$$\frac{d\widehat{T}_{u1}}{dt^*} = \left[r - p_2 B_0(n\tau^*)^+ \exp\left(-p_2 T_{u0}^*(t^* - n\tau^*)\right)\right]T_{u0}^*,$$

and thus

$$\widehat{T}_{u1}(t^*) = \widehat{T}_{u1}(n\tau^*)^+ + r T_{u0}^*(t^* - n\tau^*) - B_0(n\tau^*)^+\left(1 - \exp\left(-p_2 T_{u0}^*(t^* - n\tau^*)\right)\right).$$

Recall that this expression is only valid for $n\tau^* < t^* < (n+1)\tau^*$. Consider $\widehat{T}_{u1}((n+1)\tau^*)^-$ which is the tumor size just before the next pulse occurs at $t^* = (n+1)\tau^*$.

$$\widehat{T}_{u1}\left((n+1)\tau^*\right)^- = \widehat{T}_{u1}(n\tau^*)^+ + r T_{u0}^*\tau^* - B_0(n\tau^*)^+\left(1 - \exp(-p_2 T_{u0}^*\tau^*)\right). \quad (19)$$

Now recall that we seek the bifurcation point which separates the regions of exponential tumor growth from exponential tumor clearance. That is, we are concerned with whether the ratio of $\frac{\widehat{T}_{u1}((n+1)\tau^*)^-}{\widehat{T}_{u1}(n\tau^*)^+}$ is greater than unity (growth) or less than unity (clearance). At the transition point, we have:

$$\widehat{T}_{u1}\left((n+1)\tau^*\right)^- = \widehat{T}_{u1}(n\tau^*)^+. \quad (20)$$

Combining Eqs. (19) and (20) gives:

$$r T_{u0}^*\tau^* = B_0(n\tau^*)^+\left(1 - \exp(-p_2 T_{u0}^*\tau^*)\right). \quad (21)$$

Inserting (18) into (21), we deduce that if B_0 is periodic with period τ^* then $r T_{u0}^*\tau^* = b$.

Recalling that $\widehat{T}_{u0}(t^*) = T_{u0}^*$ and reverting to the original, dimensional variables, we deduce that at the transition point:

$$b^* = T_u(0)r\tau.$$

Thus if

$$b > b^* = T_u(0)r\tau, \quad (22)$$

then the tumor will be destroyed ($T_u \to T_u^* = 0$ as $t \to \infty$) and conversely if $b < b^*$ then the tumor will grow.

From (22), it is clear that the minimum amount of BCG required for successful treatment is directly proportional to the initial tumor size $T_u(0)$; for large values of $T_u(0)$ this becomes important in setting the treatment protocol. This prediction is in good agreement with clinical results, which show that the initial size of the tumor is a key prognostic indicator of treatment success. In particular, polyps of size greater than 3 cm, or the presence of multiple polyps (e.g., multifocal presentation of bladder cancer), are associated with poor prognosis (Meyer et al., 2002).

Figure 5 shows that our theoretical prediction of the bifurcation point (see Eq. (22)) is in good agreement with that obtained by solving the full system of equations and determining b^* numerically. This is true for large realistic values of initial tumor size $T_u(0)$ ranging from $T_u(0) = [10, 60]$ dimensionless units.
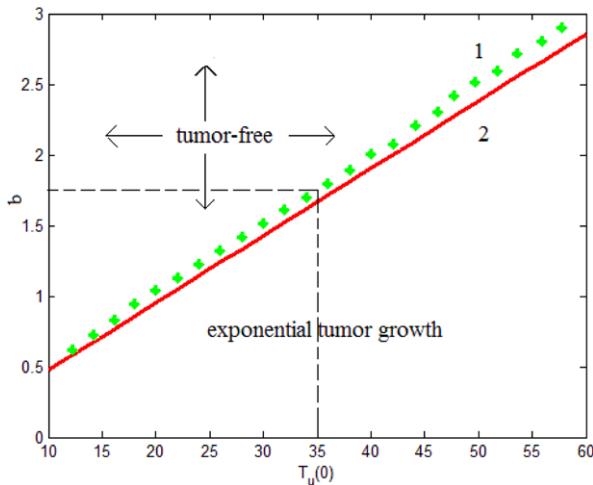
Fig. 5 Diagram showing how b^* the predicted dose of BCG needed to eliminate a tumor depends on its size $T_u(0)$ at the start of treatment: *Curve 1* (star line): threshold curve found via simulations. In the region below, the threshold curve exponential tumor growth occurs, while above it lead to the tumor elimination is predicted. For example, for $T_u(0) = 35$ (dashed line), an instillation dose with $b \geq 1.72$ will lead to a tumor-free equilibrium. *Curve 2* (solid line): theoretical estimate of threshold curve (see Eq. (22))

For example, a tumor of radius $r = 25$ mm and of depth $h = 3$ cells, will contain $T_u(0) = \pi r^2 h \times 10^6 \approx \pi \times 25^2 \times 3 \times 10^{-2} \times 10^6 = 0.6 \times 10^8$ tumor cells. The calculation is based on 1 mm^3–10^6 cells and the length of the cell being approximately 10 μm (see Bunimovich-Mendrazitsky et al., 2007). In dimensionless units (scaling rules Eq. (A.1)), this corresponds to $T'_u(0) = \frac{T_u(0)}{10^6} = 62$ and is thus considered a relatively large tumor, certainly at the upper end of the size scale. Using Eq. (22) with growth rate $r = 0.068$ and $\tau = 0.7$, we find that $b^* = 2.9$ (Fig. 5) (or, $b^* = 2.9 \times 10^6$ viable bacterial cells or colony-forming units, c.f.u.'s).

It is interesting to compare this to standard treatment used in medical practice where typical doses for weekly BCG instillation (Cheng et al., 2004) vary in the range to $2.2–6.4 \times 10^8$ c.f.u.'s. Thus, according to the above calculations, the minimum amount of BCG required to eliminate a large tumor is significantly less than the typical values used in practice. This is a real possibility that requires much further research given the ad hoc manner treatments are currently determined. Cheng et al. (2004) and Ojea et al. (2007) have already reported that current doses are likely to be too high. Note also that in our previous paper we suggested that much of the BCG leaves the bladder within the first 2 hours of instillation. Brandau (personal communication) estimates that 99% of the BCG is lost this way. A reasonable daily rate for b is thus in the range $0.01 \times (2.2–6.4 \times 10^8) = 2.2–6.4 \times 10^6$ similar to the model parameters generating Figs. 3–5.

There is good agreement between the theoretical predictions and those obtained by solving the full model numerically. Parameter values: as per Table A.1, with $\tau = 7$.

7.1. Estimating BCG administration

Using above calculations, it is possible to estimate the number of BCG instillations required to eradicate a tumor. Given the deterministic nature of the model and since it is not individual based, we must specify a small threshold tumor size below which we can consider the tumor to have been eliminated. We set the threshold arbitrarily at $T_{u\_\text{crit}} = 10^{-6}$ (which corresponds to approximately a tumor mass containing 1 cell: recall that $T_u = 1$ corresponds to a tumor containing 10^6 cells; see Appendix A).

By virtue of Eq. (10), it is possible to calculate the number N of BCG instillations, and/or the dose b, required to reach the eradication threshold. First, rearranging Eq. (10), we obtain:

$$T_u(n\tau) = T_u(0)e^{n(r\tau - p_2 b)}.$$

Setting $T_u((n+1)\tau) = T_{u\_\text{crit}} = 10^{-6}$, we can find the critical dose b_c:

$$b_c = \frac{1}{p_2}\left(r\tau - \log\left(10^{-6}/T_u(0)\right)/n\right). \tag{23}$$

In Fig. 6, we use Eq. (23) to show how b_c, the minimum dosage required to eliminate the tumor with size $T_u(0) = 60$, varies with n the number of instillations. Thus, for $n = 6$ (i.e., 6 weekly instillations), we estimate $b_c = 10.45$ and increasing the treatment schedule from 6 to 10 weeks leads to a reduction in the minimum dosage needed to achieve a cure by 41% (i.e., a reduction to $b_c = 6.34$).
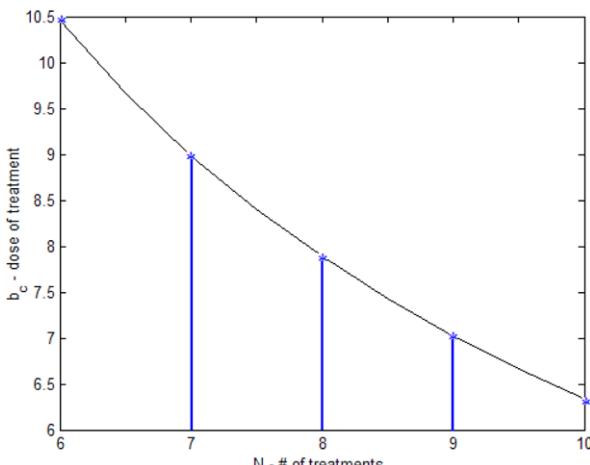

Fig. 6 The relationship obtained from Eq. (23) showing the manner in which b_c, the minimum BCG treatment dose required to eliminate a tumor of fixed size, varies with n, the number of weekly instillations administered. Parameter values: as per Table A.1, with $T_u(0) = 60$ and $\tau = 7$

8. Summary

In this paper, the complex biological processes of tumor, immune system, and BCG interactions have been modeled using a system of four differential equations and used to investigate the system's response to pulsed BCG immunotherapy. Depending on the dose (b) and the interval between treatments (τ), one of three different outcomes were obtained:

1. The "tumor-free" state, for which the tumor is completely eradicated and the BCG dynamics evolve to a limit cycle of period τ, where τ is the period of the instillations. The tumor-free state is locally stable provided the dose administrated lies within a finite range:

$$\frac{r}{p_2} < \frac{b}{\tau} < \frac{\mu}{p_4}. \tag{24}$$

2. The "tumor" state in which the tumor-free equilibrium is unstable and unbounded tumor growth is predicted. This case arises when the lower bound in Eq. (24) is violated which means that insufficient BCG is being delivered to the tumor (see Fig. 3b).
3. The "side-effect" state in which the tumor is eradicated ($T_u^* \to 0$), but the immune system is destabilized and the effector cells are in a state of growth. This case occurs when the upper bound in Eq. (24) is violated (see Fig. 3c).

The above results highlight the importance of the ratios $\frac{r}{p_2}$ and $\frac{\mu}{p_4}$ in the success of BCG immunotherapy. The former implies that it is the relative ratio between the natural growth (r) of bladder tumor cells and the BCG infection rate (p_2) that controls whether or not therapy will succeed: whichever process has the advantage, dictates whether the tumor is eradicated. Similarly, there is a competition between the rate of recruitment of effector cells (p_4) and their natural mortality rate (μ). If the rate of recruitment is high then for a given treatment protocol, the right side inequality in Eq. (24) will be violated and effector cells will accumulate.

It is interesting to compare the stability criterion for the tumor-free state when pulsed BCG is administrated with that obtained for our earlier model of continuous BCG treatment (Bunimovich-Mendrazitsky et al., 2007). Both models are identical except for the terms describing BCG entry into the bladder. In the continuous treatment, BCG enters at a constant rate b per unit time, while for the pulsed treatment a quantity b_p of BCG enters the bladder as a spike every τ time units. While for the continuous model, the tumor-free state is shown to be stable if: $\frac{r}{p_2} < b < \frac{\mu}{p_4}$, in the pulsed model the condition is just $\frac{r}{p_2} < \frac{b_p}{\tau} < \frac{\mu}{p_4}$. Thus, the two models are equivalent if we view the pulsing $\frac{b_p}{\tau}$ as the average BCG per unit time. A key difference between the models is the dynamics of the tumor-free state: with continuous treatment the tumor-free state is an equilibrium, whereas with pulsed treatment the BCG dynamics evolve to a limit cycle.

We have also shown that the response to BCG treatment depends on the initial size of the tumor and may be used to determine whether BCG treatment should be given. These model predictions confirm, Nseyo and Lamm's (1997) conclusion that the state of a patient's tumor here is an important determinant factor in deciding whether to opt for intravesical therapy.

Indeed an ultimate, but albeit still distant, application for the model is to aid in defining the appropriate rate of BCG instillation in a particular clinical situation. To achieve this goal for individual bladder cancer patients, certain clinical parameters need to be measured. Many of our model parameters were estimated from the biological and clinical literature. However, parameters such as the infection rate of the tumor cells with BCG (p_2), and the rate of stimulation of effector cells by infected tumor cells (p_4), have not yet been measured, even though they are extremely important in predicting the outcome of therapy.

In future work, we aim to develop a model that distinguishes between various types of immune cells and differences in their behavior coupled with suitable experimental data and parameter estimates. We anticipate that this will generate more accurate predictions for optimizing BCG treatments and will allow us to determine conditions under which the distinction is important. We will also investigate the effect on the system dynamics of introducing a time delay to describe the time if takes for effector cells to be recruited from the bone marrow. This delay could profoundly influence system dynamics and give a more realistic characterization of the immune response. As has been found in other applications (Mackey and Glass, 1977; Murray, 1993), the delay could profoundly influence system dynamics and give a more realistic characterization of the immune response.

In conclusion, effective treatment of bladder cancer remains a challenge despite significant improvements in preventing disease progression and improving survival. Intravesical BCG immunotherapy has been used to manage superficial transitional cell carcinoma (TCC) of the urinary bladder, to treat existing or residual tumors, to prevent tumor recurrence, and/or disease progression, and to extend patient survival. We hope that further extensions of the model presented in this paper will form the basis for future mathematical studies that will inform clinical practice.

Appendix A: Scaling of parameters

This system may be rewritten in dimensionless form, using the following scaling:

$$B' = \frac{B}{B_0}, \qquad E' = \frac{E}{E_0}, \qquad T'_i = \frac{T_i}{T_{i_0}}, \qquad T'_u = \frac{T_u}{T_{u_0}},$$

$$t' = \mu_1 t, \qquad b' = \frac{b}{\mu_1 B_0}, \qquad \beta' = \beta T_{u_0}, \qquad \alpha = \frac{\alpha}{\mu_1},$$

$$r' = \frac{r}{\mu_1}, \qquad \mu = \frac{\mu_2}{\mu_1}, \tag{A.1}$$

$$p'_1 = \frac{p_1}{\mu_1} E_0, \qquad p'_2 = \frac{p_2}{\mu_1} T_{u_0}, \qquad p'_3 = \frac{p_3}{\mu_1} E_0,$$

$$p'_4 = \frac{p_4}{\mu_1} B_0, \qquad p'_5 = \frac{p_5}{\mu_1} T_{i_0}.$$

In practice, there is a trade off between reducing parameters and retaining parameters that have operational meaning. For these reasons, we choose the scaling

$$B_0 = E_0 = T_{i_0} = T_{u_0} = 10^6 \text{ cells} \tag{A.2}$$

(similar to Kuznetsov et al., 1994). Dropping the prime notation for convenience, we obtain the dimensionless form of the model equations as stated in the main text (see Eq. (1)).

Appendix B: Floquet theory

Here, we apply Floquet theory for studying the stability of Eq. (6) which describes a linear system with periodic coefficients. A review of the theory may be found in Hartman (1964), Iooss and Joseph (1980), Guckenheimer and Holmes (1983), and Glendinning (1994). Consider the linear system of n coupled differential equations:

$$\frac{d\underline{y}}{dt} = \underline{\underline{P}}(t)\underline{y}, \tag{B.1}$$

where $\underline{\underline{P}}(t) = \underline{\underline{P}}(t + \tau)$ are periodic coefficients. Hartman (1964) has shown that there is a fundamental solution matrix of the system that can be written in the form:

$$\underline{\underline{Y}}(t) = \underline{\underline{Z}}(t) \exp(\underline{\underline{R}}t) \quad \text{with} \quad \underline{\underline{Z}}(t) = \underline{\underline{Z}}(t + \tau),$$

where $\underline{\underline{Y}}$, $\underline{\underline{Z}}$, and $\underline{\underline{R}}$ are $n \times n$ matrices and $\underline{\underline{R}}$ is a constant matrix. In particular, choosing $\underline{\underline{Y}}(0) = \underline{\underline{Z}}(0) = \underline{\underline{I}}$ gives:

$$\underline{\underline{Y}}(\tau) = \underline{\underline{Z}}(\tau) \exp(\underline{\underline{R}}\tau) = \underline{\underline{Z}}(0) \exp(\underline{\underline{R}}\tau) = \exp(\underline{\underline{R}}\tau).$$

The latter relation implies that $\underline{\underline{Y}}(n\tau) = \underline{\underline{Y}}(\tau)^n$, which in turn implies that the asymptotic behavior of $\underline{y}(t)$ depends only on the eigenvalues of $\underline{\underline{Y}}(\tau) = \exp(\underline{\underline{R}}\tau)$. In fact, $|\underline{y}(n\tau)|$ tends to zero provided all the eigenvalues of $\underline{\underline{Y}}(\tau)$ lie inside the unit circle (Glendinning, 1994). These eigenvalues are referred to as Floquet multipliers.

In practice, the fundamental matrix $\underline{\underline{Y}}$ can be constructed by finding n independent solutions: $(\underline{y}_1(t), \underline{y}_2(t), \ldots, \underline{y}_n(t))$ of system (B.1).

Appendix C: Parameter estimation

Parameter values were estimated in Bunimovich-Mendrazitsky et al. (2007) and are summarized in the following Table A.1 below.

Table A.1 List of all parameters. Note that dimensionless estimates were obtained from source values using the transformations stated in Appendix A

Parameter	Physical Interpretation (units)	Dimensional estimate (Dimensionless estimate)	Reference
μ_1	BCG half life [days^{-1}]	0.1 (1.00)	Archuleta et al. (2002)
μ_2	Effector cells mortality rate [days^{-1}]	0.041 (0.41)	Kuznetsov et al. (1994)
p_1	The rate of BCG killed by APC [cells^{-1}][days^{-1}]	1.25×10^{-7} (1.25)	Wigginton and Kirschner (2001)
p_2	Infection rate of tumor cells by BCG [cells^{-1}][days^{-1}]	0.285×10^{-6} (0.285)	Not found
p_3	Rate of destruction of infected tumor cells by effector cells [cells^{-1}][days^{-1}]	1.1×10^{-7} (1.1)	Kuznetsov et al. (1994)
p_4	Immune response activation rate [cells^{-1}][days^{-1}]	0.12×10^{-7} (0.12)	Not found
p_5	Rate of E deactivation after binding with infected tumor cells; [cells^{-1}][days^{-1}]	0.03×10^{-8} (0.003)	Kuznetsov et al. (1994)
α	Rate of E stimulation due to infected tumor cells [days^{-1}]	0.052 (0.52)	Wigginton and Kirschner (2001)
r	Tumor growth rate [days^{-1}]	0.0033 (0.033) 0.012 (0.12) 0.0068 (0.068)	Shochat et al. (1999); Swanson et al. (2003); In all simulations.
$1/\beta$	Tumor carrying capacity [cells]	$\beta = [2 \times 10^{-8} - 0.11 \times 10^{-7}]$ ($\frac{1}{\beta} = \frac{1}{[0.013, 0.022]} = [45, 76]$)	Lämmle et al. (2002); De Pillis et al. (2006)

References

Alexandroff, A.B., Jackson, A.M., O'Donnell, M.A., James, K., 1999. BCG immunotherapy of bladder cancer: 20 years on. Lancet 353, 1689.

Archuleta, J., Mullens, P., Primm, T.P., 2002. The relationship of temperature to desiccation and starvation tolerance of the Mycobacterium avium complex. Arch. Microbiol. 178, 311–314.

Bainov, D., 1993. Impulsive Differential Equations. Longman, Harlow.

Bevers, R.F.M., Kurth, K.H., Schamhart, D.H.J., 2004. Role of urothelial cells in BCG immunotherapy for superficial bladder cancer. Br. J. Cancer 91, 607–612.

Bohle, A., Brandau, S., 2003. Immune mechanisms in bacillus Calmette–Guérin immunotherapy for superficial bladder cancer. J. Urol. 170, 964969.

Bunimovich-Mendrazitsky, S., Shochat, E., Stone, L., 2007. Mathematical model of BCG immunotherapy in superficial bladder cancer. Bull. Math. Biol. Online: http://dx.doi.org/10.1007/s11538-007-9195-z

Cheng, C.W., Ng, M.T., Chan, S.Y., Sun, W.H., 2004. Low dose BCG as adjuvant therapy for superficial bladder cancer and literature review. ANz J. Surg. 74(7), 569–572.

Chopin, D., Gattegno, B., 2002. Superficial bladder tumors. Eur. Urol. 42, 533–41.

De Boer, E.C., Bevers, R.F., Kurth, K.H., Schamhart, D.H., 1996. Double fluorescent flow cytometric assessment of bacterial internalization and binding by epithelial cells. Cytometry 25, 381–387.

De Pillis, L.G., Radunskaya, A.E., Wiseman, C.L., 2005. A validated mathematical model of cell-mediated immune response to tumor growth. Cancer Res. 65(17), 7950–7958.

De Pillis, L.G., Gu, W., Radunskaya, A.E., 2006. Mixed immunotherapy and chemotherapy of tumors: modeling, applications and biological interpretations. J. Teor. Biol. 238, 841–862.

Durek, C., Brandau, S., Ulmer, A.J., Flad, H.D., Jocham, D., Bohle, A., 1999. Bacillus Calmette–Guérin (BCG) and 3D tumors: an in vitro model for the study of adhesion and invasion. J. Urol. 162, 600–605.

Glendinning, P., 1994. Stability, Instability and Chaos: An Introduction to the Theory of Nonlinear Differential Equations. Cambridge University Press, Cambridge.

Guckenheimer, J., Holmes, P., 1983. Nonlinear Oscillations, Dynamical Systems, and Bifurcations of Vector Fields. Springer, New York.

Hartman, P., 1964. Ordinary Differential Equations. Wiley, New York.

Iooss, G., Joseph, D., 1980. Elementary Stability and Bifurcation Theory. Springer, New York.

Kim, J.C., Steinberg, G.D., 2001. The limits of bacillus Calmette–Guerin for carcinoma in situ of the bladder. J. Urol. 165(3), 745–756.

Kirschner, D., Panetta, J., 1998. Modelling immunotherapy of the tumor-immune interaction. J. Math. Biol. 37(3), 235–252.

Kuznetsov, V.A., Makalkin, I.A., Taylor, M.A., Perelson, A.S., 1994. Nonlinear dynamics of immunogenic tumours: parameter estimation and global bifurcation analysis. Bull. Math. Biol. 56, 295–321.

Lakmeche, A., Arino, O., 2001. Nonlinear mathematical model of pulsed therapy of heterogeneous tumors. Nonlinear Anal. R. World Appl. 2, 455–465.

Lakshmikantham, V., Bainov, D.D., Simeonov, P.S., 1989. Theory of Impulsive Differential Equations. World Publishers, Singapore.

Lämmle, M., Beer, A., Settles, M., Hanning, C., Schwaibold, H., Drews, C., 2002. Reliability of MR imaging-based virtual cystoscopy in the diagnosis of cancer of the urinary bladder. Am. J. Roentgenol. 178, 1483–1488.

Mackey, M., Glass, L., 1977. Oscillation and chaos in physiological control systems. Science 197, 287–289.

Meyer, J.P., Persad, R., Gillatt, D.A., 2002. Use of bacille Calmette–Guérin in superficial bladder cancer. Postgrad. Med. J. 78, 449–454.

Murray, J.D., 1993. Mathematical Biology, 2nd edn. Springer, London.

Nseyo, U.O., Lamm, D.L., 1997. Immunotherapy of Bladder Cancer. Sem. Surg. Oncol. 13, 342–349.

Ojea, A., Nogueira, J.L., Solsona, E., et al., 2007. A multicentre, randomized prospective trial comparing three intravesical adjuvant therapies for intermediate-risk superficial bladder cancer: low-dose bacillus Calmette–Guérin (27 mg) versus very low-dose bacillus Calmette–Guérin (13.5 mg) versus mitomycin C. Eur. Urol. 52, 1398–406.

Panetta, J., 1996. A mathematical model of periodically pulse chemotherapy: tumor recurrence and metastasis in a competition environment. Bull. Math. Biol. 58, 425–447.

Patard, J.J., Saint, F., Velotti, F., Abbou, C.C., Chopin, D.K., 1998. Immune response following intravesical bacillus Calmette–Guérin instillations in superficial bladder cancer: a review. Urol. Res. 26(3), 155–159.

Schenk-Braat, E.A.M., Bangma, C.H., 2005. Immunotherapy for superficial bladder cancer. Cancer Immunol. Immunother. 54(5), 414–423.

Shulgin, B., Stone, L., Agur, Z., 1998. Pulse vaccination strategy in the SIR epidemic model. Bull. Math. Biol. 60, 1–26.

Stone, L., Shulgin, B., Agur, Z., 2000. Theoretical examination of the pulse vaccination policy in the SIR epidemic model. Math. Comput. Mod. 31(4–5), 207–215.

Schenkman, E., Lamm, D.L., 2004. Superficial bladder cancer therapy. Sci. World 4, 387–399.

Shochat, E., Hart, D., Agur, Z., 1999. Using computer simulations for evaluating the efficacy of breast cancer chemotherapy protocols. Math. Models Methods Appl. Sci. 9(4), 599–615.

Swanson, K.R., Bridge, C., Murray, J.D., Alvord, E.C., 2003. Virtual and real brain tumors:using mathematical modeling to quantify glioma growth and invasion. J. Neurol. Sci. 216, 1–10.

Zlotta, A.R., van Vooren, J.P., Huygen, K., et al., 2000. What is the optimal regimen for BCG intravesical therapy? Eur. Urol. 37, 470.

Zwillinger, D., 1989. Handbook of Differential Equations. Academic Press, New York.

Wigginton, J., Kirschner, D., 2001. A model to predict cell-mediated immune regulatory mechanisms during human infection with Mycobacterium tuberculosis. J. Immunol. 166, 1951–1967.